Large-Scale Drivers of Tropical Extreme Precipitation Events: The Example of French Overseas Territories

Erwan Cornillault, Philippe Peyrille, Fleur Couvreux, Romain Roehrig

Geophysical Research Letters

RESEARCH LETTER
10.1029/2024GL108770

Large-Scale Drivers of Tropical Extreme Precipitation Events: The Example of French Overseas Territories

Erwan Cornillault[1], Philippe Peyrille[1], Fleur Couvreux[1], and Romain Roehrig[1]

[1]Centre National de Recherches Météorologiques, Université de Toulouse, Météo-France, CNRS, Toulouse, France

Key Points:

- Over most of the studied tropical small islands, only 10%–30% of extreme precipitation events occur near a tropical storm or cyclone
- Tropical storms and cyclones favor heavier rainfall and raise the probability of occurrence of extreme precipitation by a factor of 4–15
- The other largest part of events occur in a large-scale, intense, moist, and convective anomaly driven mainly by the intraseasonal timescale

Supporting Information:

Supporting Information may be found in the online version of this article.

Correspondence to:

E. Cornillault,
erwan.cornillault@meteo.fr

Citation:

Cornillault, E., Peyrille, P., Couvreux, F., & Roehrig, R. (2024). Large-scale drivers of tropical extreme precipitation events: The example of French overseas territories. *Geophysical Research Letters*, *51*, e2024GL108770. https://doi.org/10.1029/2024GL108770

Received 22 FEB 2024
Accepted 24 JUL 2024

Author Contributions:

Conceptualization: Erwan Cornillault, Philippe Peyrille, Fleur Couvreux, Romain Roehrig
Data curation: Erwan Cornillault, Philippe Peyrille
Formal analysis: Erwan Cornillault, Philippe Peyrille, Fleur Couvreux, Romain Roehrig
Investigation: Erwan Cornillault, Philippe Peyrille, Fleur Couvreux, Romain Roehrig
Methodology: Erwan Cornillault, Philippe Peyrille, Fleur Couvreux, Romain Roehrig
Resources: Philippe Peyrille
Software: Erwan Cornillault

Abstract Due to their severity and lack of predictability, understanding and forecasting extreme precipitation events (EPEs) is critical for disaster risk reduction. The present work documents the large-scale environment of tropical EPEs based on a 42-year data set combining dense rain-gauge networks that cover several tropical small islands and coastal regions. Approximately 10%–30% of EPEs are associated with a tropical storm or cyclone (TC), except for Reunion, for which its high topography makes it reach 55%. TCs multiply the EPE probability by a factor of 4–15, especially during TCs of category 1 or higher. A composite analysis demonstrates that the remaining large part of EPEs occurs within large-scale and strong moist, convective, and cyclonic wind anomalies resulting from the superimposition of intraseasonal, seasonal-to-annual, and interannual timescales. These intense anomalies come essentially from intraseasonal variability, and lower frequencies improve the effect of intraseasonal events in creating a favorable environment for EPEs.

Plain Language Summary Floods and landslides, mainly caused by extreme precipitation events (EPEs), are severe disasters that affect populations and economies. However, their prediction, especially in tropical areas, is challenging. Here, we study the main atmospheric configurations leading to EPEs using rain-gauge data densely sampling several tropical small islands and coastal regions, covering the period 1979–2021. In areas prone to tropical storms and cyclones (TCs), these systems account for 10%–30% of EPEs, except for Reunion, whose high topography increases it up to 55%. TC-related EPEs are also more intense than non-TC-related EPEs. TCs multiply the EPE probability of occurrence by 4–15 times, depending on the region and the TC category. Non-TC-related EPEs are shown to occur within specific large-scale weather patterns in which moisture is highly increased, and convective storms are more active. These patterns involve phenomena occurring at intraseasonal (2–90-day periods), seasonal-to-annual (91–365-day periods), and interannual (periods above one year) timescales. The intraseasonal variability helps the most to develop this environment favorable to the occurrence of EPEs. Slower signals build a background on which intraseasonal variability can have more effects. The real-time monitoring of these different features should improve EPE forecasting capabilities and deliver more early warnings.

1. Introduction

In the tropical belt, mesoscale convective systems provide the majority of precipitation (e.g., Roca et al., 2014). Especially, long-lived MCSs (Roca & Fiolleau, 2020) or highly organized ones (Dai & Soden, 2020; Semie & Bony, 2020) bring heavy rainfall in a short period, often within a day, resulting in Extreme Precipitation Events (EPEs) associated with extensive socio-economic damages (CRED and UNDRR, 2020). Anticipating EPEs at the weather scale is thus a priority for disaster risk reduction policies, but their forecast still remains uncertain (e.g., MacLeod et al., 2021; Vogel et al., 2020; Woodhams et al., 2018). A better understanding of the large-scale environment of EPEs may help to identify at-risk areas several days in advance.

One of these predictors can be tropical storms and cyclones (referred to as TCs hereafter). Few studies quantified the TC contribution to EPEs at the scale of the tropics. Among them, based on satellite precipitation estimates, Prat and Nelson (2016) found that 13%–31% of EPEs can be associated with TCs in the areas where the latter are active with large geographical disparities. Zhao (2022) indicates a global average of 6.9%. Regional studies are more common in the literature, as for the United States (e.g., Knight & Davis, 2009; Kunkel et al., 2010), Australia (e.g., Khouakhi et al., 2017; Villarini & Denniston, 2016), Japan (e.g., Khouakhi et al., 2017) or Southwest Pacific Ocean islands (e.g., Deo et al., 2021; Pariyar et al., 2020). Moreover, informal discussions with Météo-France forecasters operating in the French overseas territories emphasize that TCs likely enhance the

Supervision: Philippe Peyrille, Fleur Couvreux, Romain Roehrig
Validation: Philippe Peyrille, Fleur Couvreux, Romain Roehrig
Visualization: Erwan Cornillault
Writing – original draft: Erwan Cornillault
Writing – review & editing: Philippe Peyrille, Fleur Couvreux, Romain Roehrig

occurrence probability of EPEs. Deo et al. (2021) find such a relationship in the Southwest Pacific Ocean, but this modulation remains to be assessed at the scale of the tropics.

However, although these studies generally differ regarding EPE definitions, considered data sets, and EPE-TC association methods, they all agree that TCs are not the main contributors to EPE occurrence in the tropical belt, except for very specific areas. Another key large-scale ingredient is Precipitable Water (PW), which positively correlates with EPE occurrence, as found in the United States (Kunkel et al., 2020) and at a more global scale (e.g., Kim et al., 2022; Roderick et al., 2019, 2020). The processes driving this moist environment of EPEs involve various timescales. At the interannual timescale, the variability of sea surface temperatures alters the atmospheric circulation and the convective environment, thereby modulating the probability of EPE occurrence. These modes of variability include El Niño–Southern Oscillation (ENSO—Pariyar et al., 2020), the Indian Ocean Dipole (IOD—Ajayamohan & Rao, 2008), the Southern Indian Ocean Dipole (SIOD—Hoell & Cheng, 2018; Rapolaki et al., 2019), or those in the Atlantic Ocean (Muller et al., 2008; Ta et al., 2016). Then, only a few recent studies emphasized the role of the intraseasonal variability (defined here by scales from synoptic to planetary scales, Serra et al., 2014). EPE occurrence is favored by intraseasonal circulations driving anomalous moist and convective conditions, as, for instance, during the passage of a Madden-Julian Oscillation disturbance (MJO—Schreck, 2021), or of an intense convectively-coupled equatorial wave (CCEW—Ferrett et al., 2020). The interaction between several CCEWs has also been found relevant to EPEs (Lafore et al., 2017; Latos et al., 2021; Lubis & Respati, 2021; Peyrillé et al., 2023), as well as tropical-extratropical interactions (Pariyar et al., 2020; Rapolaki et al., 2019). However, a tropics-wide view of the atmospheric conditions leading to EPEs is still lacking.

The present study has two main objectives. First, we assess the TC contribution to EPE occurrence, particularly quantifying the increase in EPE occurrence probability during TCs. Second, we identify the key large-scale patterns and time scales associated with non-TC EPEs. Most of the previous studies on tropical EPEs—related to TCs or not—used satellite products, providing global coverage despite known bias and discrepancies in their detection of EPEs (Alexander et al., 2019, 2020; Prat & Nelson, 2013; Sanogo et al., 2022). We use the Météo-France rain gauge network deployed in the tropical French overseas territories to overcome this limitation. This rich data set samples most tropical ocean basins and one coastal domain (Figure 1, Figures S1 and S2 in Supporting Information S1).

2. Data Sets and Methods

2.1. Definition and Detection of Extreme Precipitation Events

This study focuses on the 13 main tropical French overseas departments and territories (referred to as territories hereafter). Except for French Guiana (the only continental area in South America), the study considers islands or archipelagos distributed along the tropical ocean basins with Reunion and Mayotte in the Southwest Indian Ocean; New-Caledonia (NC) and Wallis & Futuna (WF) in the Southwest Pacific; French Polynesia in the Central Pacific, divided into five main archipelagos (Society, Marquesas, Tuamotu, Gambier, and Austral Islands); and Martinique, Guadeloupe, and St-Barthelemy (French West Indies, FWI) in the Atlantic Ocean (Figure 1). Their location along the tropical belt at different latitudes allows us to sample a diversity of climates ranging from subtropical climate (Reunion, NC, and Austral Islands) to deep equatorial climate for domains located near the Intertropical Convergence Zone (French Guiana, Mayotte) and the South Pacific Convergence Zone (WF, Brown et al., 2020). FWI and the rest of French Polynesia are transition areas between these climates.

The daily rainfall records come from a large and relatively dense network of rain gauges provided by Météo-France covering 42 years, from 1979 to 2021. Missing data are left unfilled, and only rain gauges with less than 5% missing data are retained (156 in total, each territory containing between 1 and 37 rain gauges, some of which sample the sharp relief of certain territories, Figure 1, Figures S1 and S2 in Supporting Information S1). EPEs are identified for each rain gauge as the days when rainfall exceeds the 99th all-day percentile (hereafter p99). Each rain gauge thus records between 150 and 160 EPEs. The p99 median values range between 35 and 90 mm d^{-1} across the different territories (Figure 1), with geographic disparities depending on the location and spatial sampling by rain gauges (Figure S2 in Supporting Information S1). P99 is relatively spatially homogeneous for most territories except for islands with high topography (Reunion, NC, FWI).

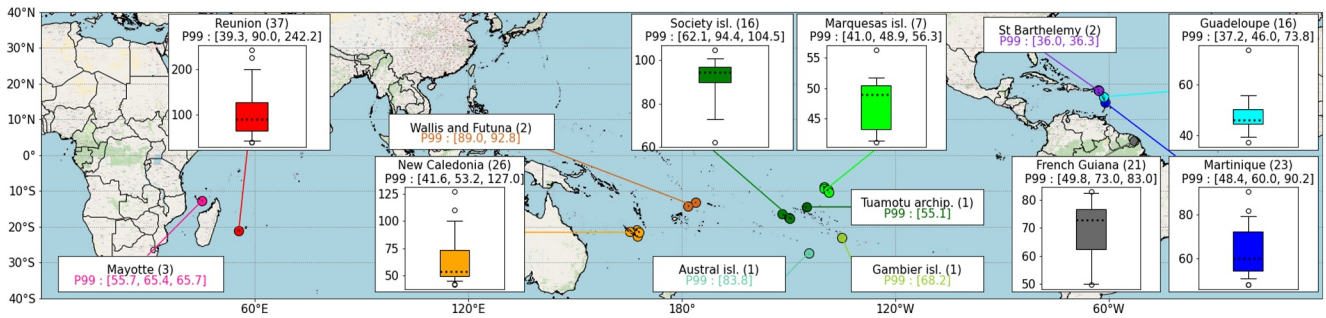

Figure 1. Rain-gauge networks and p99 values used in this study. Titles show the number of rain gauges per territory. If three or fewer rain gauges are available, the p99 is given directly. For more rain gauges, a box-and-whisker plot shows the p99 distribution (dotted line: median, box limits: first and third quartiles, whiskers: 5th and 95th percentiles, flyer points: data outside whiskers). Titles also indicate the median p99, with min and max in square brackets.

2.2. Cyclonic Versus Non-Cyclonic EPEs

EPEs are separated between those associated with a TC at any stage (cyclonic EPEs) and the others, named non-cyclonic EPEs. TCs are identified with the International Best Track Archive For Climate Stewardship data set (IBTrACS—Knapp et al., 2010) for 1979–2021. TCs are then classified according to wind gust speeds using the Saffir-Simpson Hurricane Scale, with some systems not classified because of missing wind data. Spurs systems are excluded.

For a given rain gauge, cyclonic days are first defined generically as days with at least one TC located within a 1,000-km distance. Cyclonic EPEs are then determined by the co-occurrence of an EPE and a cyclonic day. A 500-km threshold is often used in the literature (e.g., Deo et al., 2021; Prat & Nelson, 2016), but larger distances are also frequent (e.g., Bagtasa, 2017; Zhao, 2022) because heavy rainfall can be triggered rather far away from the TC's center due to modifications of the large-scale environment (e.g., Chen, 2012). Here, 1,000 km is chosen based on a sensitivity study of the cyclonic EPE number to this distance (Figure S3 in Supporting Information S1). For all territories, the fraction of cyclonic EPEs shows an asymptotic behavior for distances above 1,000 km, suggesting a reduced link between TCs and EPEs beyond this distance. Besides, the following results are weakly sensitive to the chosen threshold (see Figures S4 and S5 in Supporting Information S1 for 500 and 1,500-km distances).

We then quantify the fraction of cyclonic EPEs over all EPEs and the contribution of each TC category to this fraction. Following Peyrillé et al. (2023), the influence of TCs on EPEs is quantified by the change in EPE frequency of occurrence caused by TCs:

$$\Delta P_{EPE,c}(cat) = \frac{P_{EPE,c}(cat) - P_{EPE}}{P_{EPE}} \quad (1)$$

where P_{EPE} is the frequency of EPE occurrence (0.01 by definition), and $P_{EPE,c}$ is the conditional probability of observing a cyclonic EPE. For a given TC category and rain gauge, $P_{EPE,c}$ is given by the ratio of cyclonic EPEs corresponding to the TC category to the number of cyclonic days within the same category. So, $P_{EPE,c}$ gives a full account of the diversity of TC climatology among territories. $\Delta P_{EPE,c}(cat) > 0$ indicates an increased probability of EPE occurrence when this TC category is present. The assessment of its statistical significance is described in the Supporting Information (Text S2 in Supporting Information S1). $\Delta P_{EPE,c}(cat)$ is set to -1 when no EPE occurs for a given TC category.

2.3. Large-Scale Environment of Non-Cyclonic EPEs

The large-scale atmospheric conditions associated with non-cyclonic EPEs are documented using daily means of PW and 850-hPa wind from the ECMWF Reanalysis v5 (ERA5) data set (Hersbach et al., 2020, 0.25° horizontal resolution). Daily averaged outgoing longwave radiation (OLR) data derived from the National Oceanic and Atmospheric Administration (NOAA) polar-orbiting satellites (Liebmann & Smith, 1996, 2.5° horizontal resolution) provide a large-scale proxy for deep convective activity. Their respective anomalies are determined by subtracting the daily 1979–2021 climatology from the raw daily value. The contributions of the intraseasonal (2–

90-day periods), seasonal-to-annual (91–365-day periods), and interannual (above 365 periods) timescales to the total anomaly are then assessed using a Lanczos temporal band- or low-pass filtering (Duchon, 1979).

In the same logic as cyclonic EPEs, computations about non-cyclonic EPEs (composite maps and PDFs) are realized for each rain gauge separately. The average over all rain gauges of a given territory is then presented. The composite of non-cyclonic EPEs is defined for a given territory as the average of the non-cyclonic EPEs for all its rain gauges. The probability density function (PDF) of a given variable at a given rain gauge, either for its climatology or conditioned to non-cyclonic EPE days, is computed using the nearest grid point and at the daily timescale. The assessment of composite and PDF statistical significance is explained in Supporting Information (Text S2 in Supporting Information S1).

3. Contribution of Tropical Cyclones on EPEs

The TC contribution to EPE occurrence is illustrated in Figure 2a. The territory averages vary from a few percent in French Guiana (not considered hereafter), Marquesas, Tuamotu, Gambier, and Australs islands to 10%–30% in most domains and up to 55% in Reunion. This geographical distribution matches the average TC contribution to total rainfall (Figure S6a in Supporting Information S1) and coincides with the climatological occurrence of TCs (Figure S6b in Supporting Information S1). Territories with the largest fraction of cyclonic days show the highest fractions of EPEs. The sub-territory spread is relatively small (around 10%) except for Reunion (50%), where the TC contribution rises to 60%–80% in the mountainous area (not shown). Indeed, the Reunion's relief shows higher rainfall intensity during cyclonic days than on coasts (Figure S6c in Supporting Information S1). This role of topography may be general, but the sparse rain gauge network of the other territories does not allow it to be fully captured (see Text S1 and Figures S1 and S2 in Supporting Information S1). In Pointe-à-Pitre (Guadeloupe) and Fort-de-France (Martinique), the fraction of cyclonic EPEs aligns with Prat and Nelson (2016) (15%–25%, see their Table 2). However, results are about twice as high for St-Denis (Reunion) and even higher for Noumea (NC), possibly due to the use of rain gauges instead of satellite products. Cyclonic EPEs are also more intense than non-cyclonic EPEs (see Figure S7 in Supporting Information S1), especially over the Reunion's relief.

Figure 2b examines the contribution of each TC category to cyclonic EPEs. Tropical storms (TSs) are the leading contributors, accounting for 40%–60% of cyclonic EPEs across most territories and up to 80% in areas with fewer cyclonic EPEs. This large contribution reflects the TS climatological higher frequency (35%–50% of cyclonic days, not shown). The contribution of other TC categories is more diverse across the territories.

Figure 2c further quantifies the modulation of EPE probability of occurrence during cyclonic days ($\Delta P_{EPE,c}$, see Section 2.2). Except for WF and some French Polynesian archipelagos, $\Delta P_{EPE,c}$ is significantly positive, with large values (3–14 for a TC of any category, blue). It indicates a significant 4 to 15-fold increase in the EPE probability of occurrence (P(cat)/P) if a TC of any category is near a rain gauge, even though such a configuration is relatively rare. Due to their predominant occurrence, the modulation of EPE occurrence by the TS category is close to that considering all categories. $\Delta P_{EPE,c}$ increases from TS to more intense TC in most territories. However, there is no consistent increase in EPE probability of occurrence with the strongest categories across the territories. Society Islands exhibit quite an extreme behavior for the strongest TCs (categories 2 and 3+, 20-fold increase), such as in the Marquesas islands for the TS category. These results must be taken with caution as TCs events, despite their significant $\Delta P_{EPE,c}$, remain rare, especially the strongest ones.

To summarize, although TCs are rare events, their proximity to a given location efficiently favors the triggering of EPEs, with a 4 to 15-fold increase of the EPEs probability. Cyclonic EPEs are generally more intense than non-cyclonic EPEs. Except for Reunion, they contribute to 10%–30% of total EPEs with a leading contribution from TS.

4. Atmospheric Conditions During Non-Cyclonic EPEs

We first examine the meteorological drivers of non-cyclonic EPEs over Reunion. These events are characterized by a large-scale moist (+10 kg m^{-2}) and convective (observed with negative OLR anomaly, −43 W m^{-2}) anomaly centered on the island spanning about 2,000–2,500 km (Figure 3a). Two dry anomalies surround the moist one, a small one southwest of the island and another, larger and stronger (around −3 kg m^{-2} and 8 W m^{-2}), between Australia and the Maritime Continent. The moist pattern is associated with cyclonic low-level anomalous circulation southwest of the island, with a northwest anomalous wind around 5 m s^{-1} over Reunion, bringing

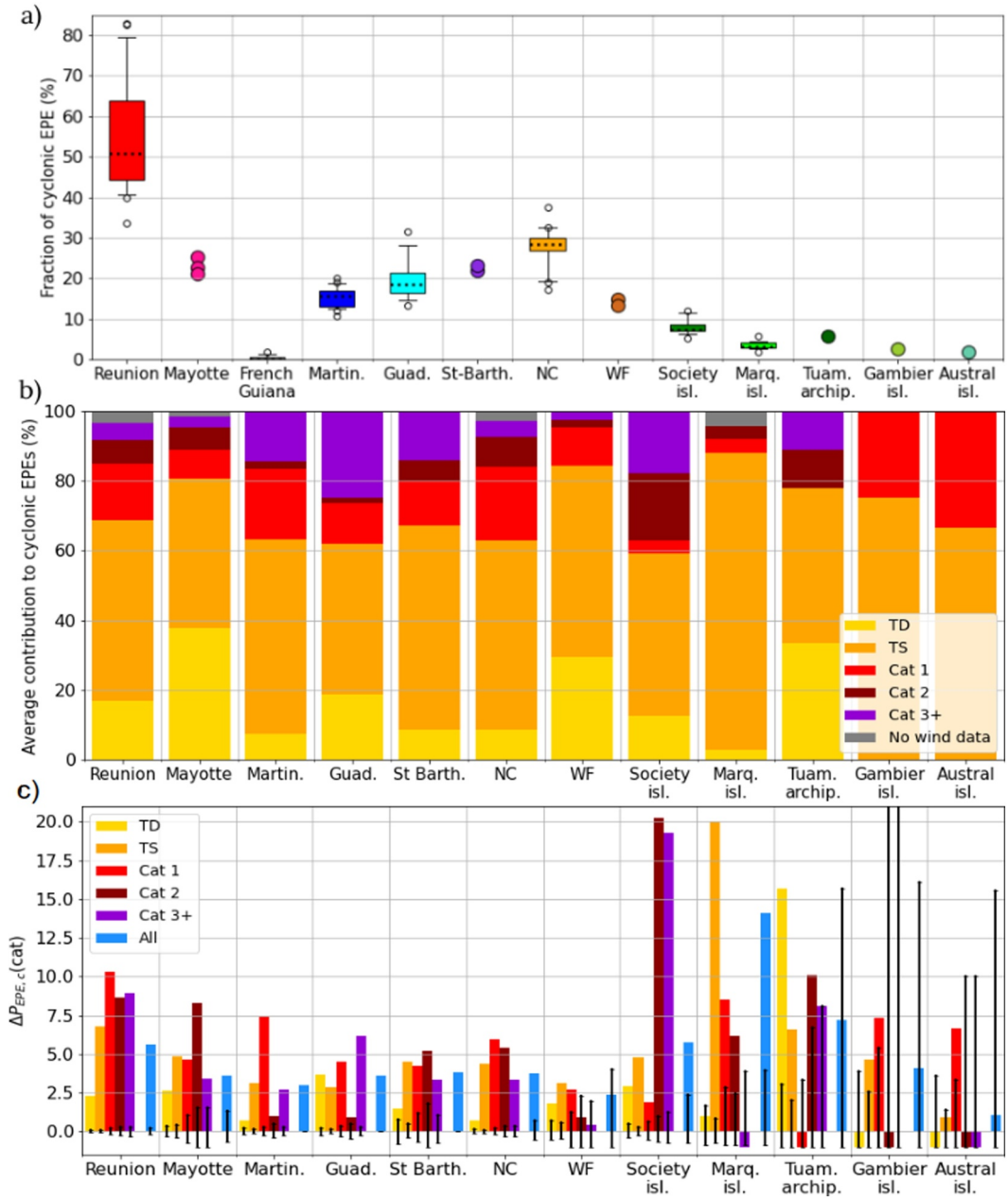

Figure 2. For each territory, (a) distribution across its rain-gauge network of the cyclonic extreme precipitation event (EPE) fraction over all EPEs (same boxplots as in Figure 1), (b) fraction of cyclonic EPEs by TC category, and (c) change in EPE frequency of occurrence ($\Delta P_{EPE,c}$, with black lines indicating significance thresholds). (b, c) are averaged over the territory rain-gauge network for each TC category (yellow-to-red scale, with gray for TCs without wind data (b) and blue for all TCs (c)). French Guiana is excluded for (b) and (c) due to very rare cyclonic EPEs.

moister air from the equator. Two anticyclonic circulations are also present, one large, around 80°E, and the other narrower, 25° south of Reunion. On a larger scale, anomalous easterlies dominate the center of the Indian Ocean, linked to a divergent circulation centered on the Maritime continent, consistent with the second dry anomaly. Anomalous westerlies and moist and convectively active anomalies cover the western and central equatorial Pacific Ocean (around +2 kg m^{-2} and −6 W m^{-2}).

Figures 3b–3d separates the previous anomalies into intraseasonal, seasonal-to-annual, and interannual components. The intraseasonal scale primarily explains the signal over the Indian Ocean, showing similar dry/wet anomalies to total anomalies (+8 kg m^{-2} and −40 W m^{-2} over Reunion, Figure 3b). The southern vortices likely

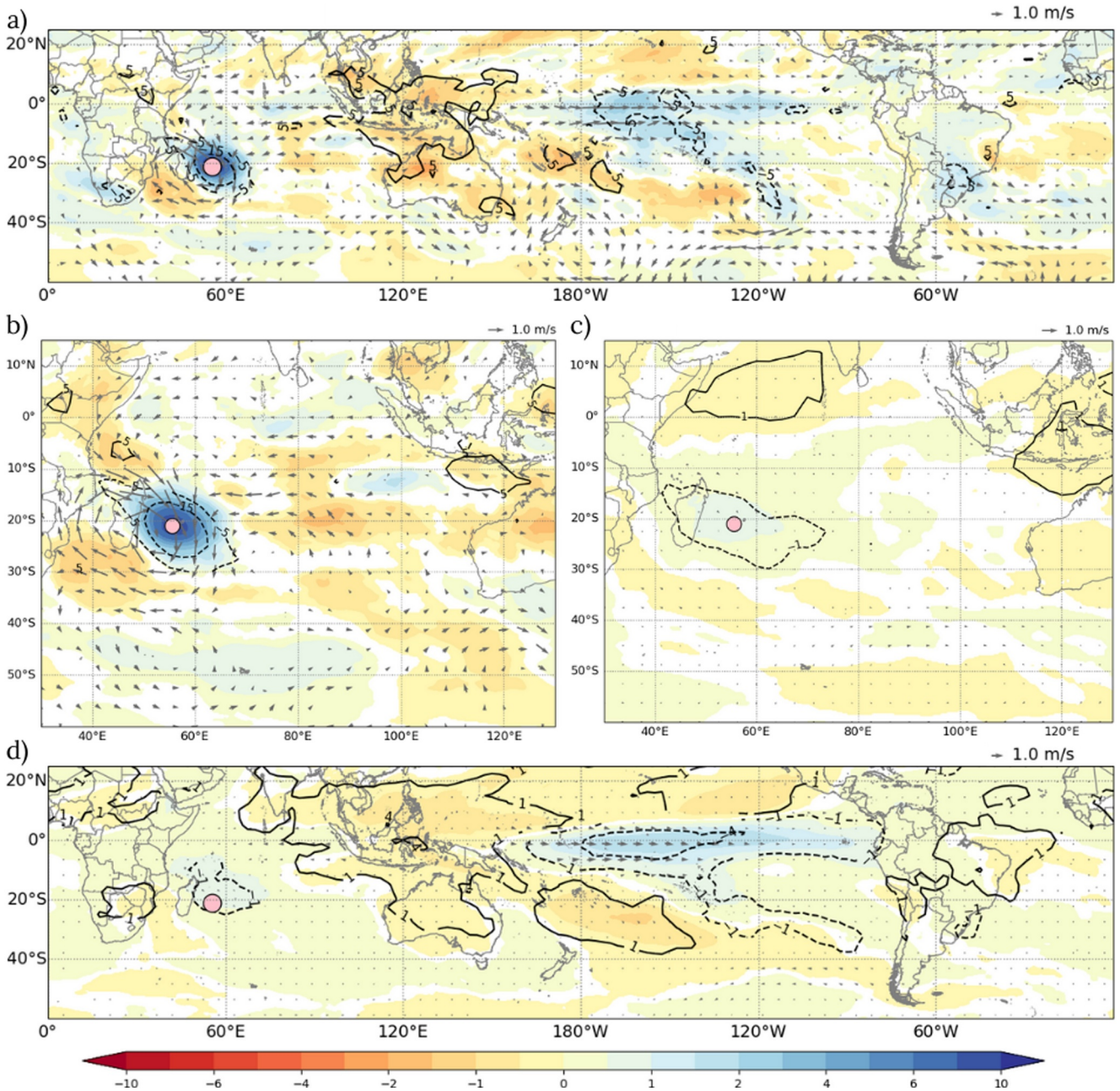

Figure 3. (a) Reunion non-cyclonic extreme precipitation events composite anomalies of Precipitable Water (shading), outgoing longwave radiation (OLR, black contours, for absolute values of 5, 15, and 40 W m^{-2}, negative values in dotted lines), and 850-hPa wind (gray arrows). (b, c, d) Same as (a) but showing contributions of intraseasonal, seasonal-to-annual, and interannual timescales (same OLR contours in panel (b) as in panel (a) and in panels (c, d) contours for absolute values of 1 and 4 W m^{-2}) respectively. Only statistically significant values at the 95% confidence level are displayed. Reunion is depicted with a pink dot.

result from mid-latitude Rossby waves, while a CCEW (Kiladis et al., 2009) may reinforce the PW dipole between 60°E and 90°E, with anomalous easterlies between the equator and 20°S. Although statistically significant, the seasonal-to-annual and interannual signals (Figures 3c and 3d) are about one order of magnitude weaker than the intraseasonal contribution. Nevertheless, they still influence the large-scale moist/convective environment of EPEs. The interannual contribution controls the divergent circulation centered on the Maritime Continent flanked by increased convection/humidity in the Central Pacific and Indian Oceans (Figure 3d). This pattern resembles an El Niño phase (McPhaden et al., 2020). At a shorter spatial scale, the West/East dipole of PW and OLR in the Indian Ocean bears similarities with a positive IOD phase (Saji et al., 1999). The seasonal-to-annual anomalies,

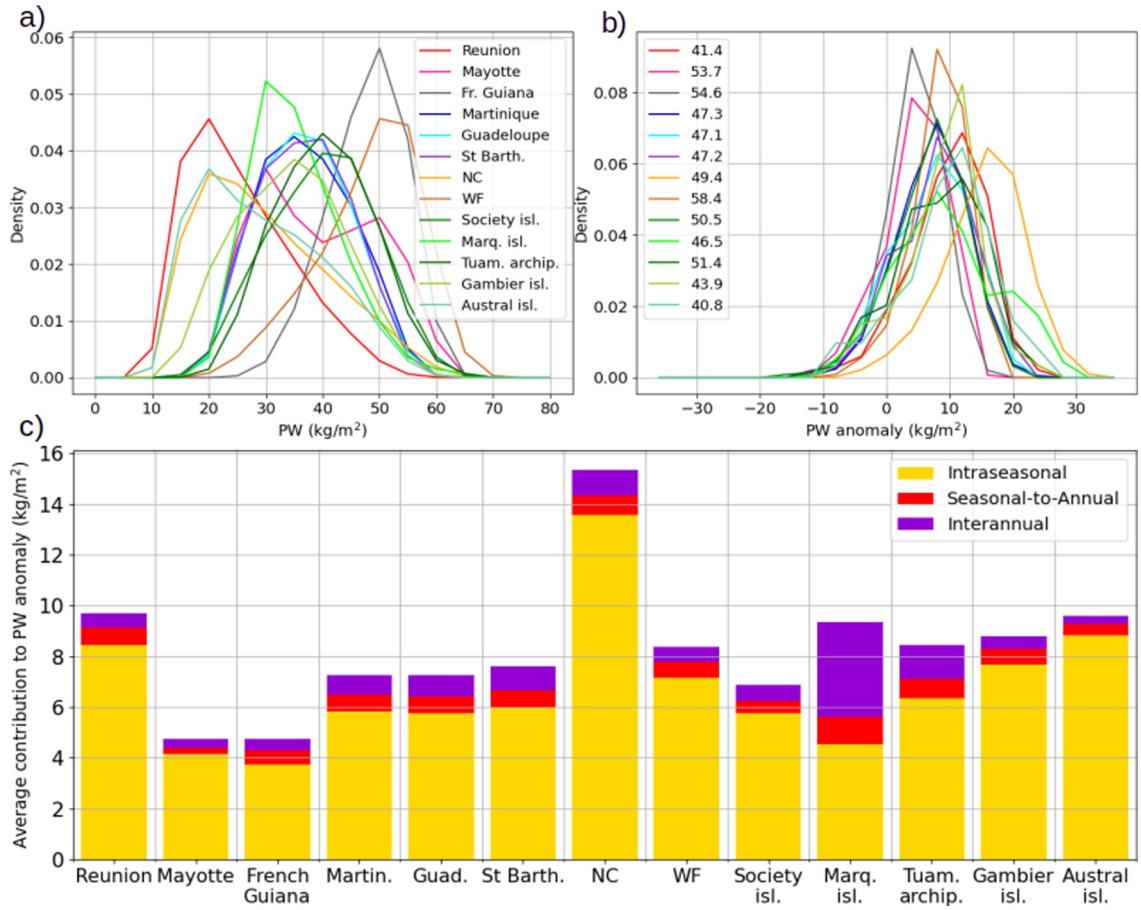

Figure 4. PDFs of Precipitable Water (PW) for (a) the all-year-round daily climatology (5-kg m^{-2} bins), (b) during non-cyclonic extreme precipitation events (EPEs) only (4-kg m^{-2} bins) for each territory (see Section 2.3 for computation details). (c) Mean contributions of intraseasonal, seasonal-to-annual, and interannual timescales to the total PW anomalies occurring during non-cyclonic EPEs. The legend in panel (b) indicates the mean values of PW (kg m^{-2}) during non-cyclonic EPEs for each territory.

even smaller, are characterized by a zonal dipole of PW/OLR across the Indian Ocean (Figure 3c), similar to an SIOD pattern (Behera & Yamagata, 2001), and a meridian one between Reunion and the Arabian Sea.

Composite maps of total anomalies are provided for other territories in Supporting Information (Figures S8 and S9 in Supporting Information S1). While PW and OLR anomalies vary across territories (e.g., the presence or not of mid-latitudes Rossby waves or CCEWs, the phase of ENSO, …), non-cyclonic EPEs always occur within a large-scale and intense moist and convective anomaly—shown as positive PW and negative OLR signals—associated with low-level cyclonic vorticity, resulting in an anomalously moist flow from equatorial regions.

We now document the timescales and magnitudes of PW anomalies that consistently accompany non-cyclonic EPEs to emphasize commonalities and differences among territories. Climatological PW distributions (Figure 4a) further confirm that our data set samples a variety of tropical climates (modal values from 20 kg m^{-2} to 50 kg m^{-2}), clustered into three groups. The driest territories (Reunion, NC, and Austral Islands) are in subtropical regions where cooler sea surface temperatures and large-scale subsidence occur, consistently leading to a dry environment. French Guiana and WF are the moistest territories, located within the deep tropics. FWI and the rest of French Polynesia show more symmetric PDFs with intermediate modal values (30–40 kg m^{-2}). Mayotte uniquely exhibits a bimodal PDF, corresponding to a marked seasonality between its dry and wet seasons.

Non-cyclonic EPEs coincide with the highest PW values of climatological PDFs. Average PW values (see numbers in Figure 4b legend) correspond at least to the 82nd percentile of climatological PDFs in the Austral islands until the 91st percentile in NC. Despite different climatological PW distributions between territories, those

of PW anomalies occurring during non-cyclonic EPEs exhibit very similar features. As emphasized above, most non-cyclonic EPEs arise within a moist anomaly (Figure 4b, from 82% in Mayotte to 97% in NC, not shown). Modal values of the PW anomaly distribution vary from 4 (French Guiana and Mayotte) to 16 kg m^{-2} over NC (Figure 4b). Maximum PW anomalies can reach 20 kg m^{-2} in most territories except in the deep tropics, likely due to a climatological environment already near saturation. Consistently with composite maps, the 850-hPa wind direction PDFs show anomalous poleward wind during non-cyclonic EPEs (Figures S10 and S11 in Supporting Information S1). Note that the wind's local-scale influence can be important during non-cyclonic EPEs (e.g., Aoki & Shige, 2023; Wang & Sobel, 2017), although not investigated here since we focus on large-scale drivers.

Figure 4c quantifies the contribution of the different timescales to the intense composite PW anomaly observed during non-cyclonic EPEs, whose average values also correspond to the highest percentiles. It highlights the significant intraseasonal contribution to the intense moist environment of non-cyclonic EPEs in all territories (from almost 4 kg m^{-2} in French Guiana to 14 kg m^{-2} in NC). The seasonal-to-annual and interannual timescales have weaker contributions, though statistically significant (on average less than 1 kg m^{-2}). A stronger interannual contribution can be noticed in the Marquesas islands (almost 4 kg m^{-2}), likely because of the strong ENSO signal in the Central Pacific (coherent with Figure S9 in Supporting Information S1 depicting a strong ENSO pattern in total anomalies).

To summarize, non-cyclonic EPEs are most frequently associated with a large-scale intense moist anomaly dominated by intraseasonal timescales. This presence of strong intraseasonal and total anomalies is specific to non-cyclonic EPEs, whereas the relatively large contribution of intraseasonal scale is a climatological feature (not shown). The same analysis conducted for OLR (Figure S12 in Supporting Information S1) indicates that the convective anomaly during non-cyclonic EPEs is also a large-scale feature mainly driven by intense intraseasonal variability.

5. Conclusion

Based on long records (1979–2021) from dense rain-gauge networks covering several small tropical islands and one coastal region, the present paper documents EPEs over a wide range of tropical climates. Our data set provides a tropics-wide view of EPEs, sampling various climates, but it advantageously does not rely on satellite observations, which exhibit large uncertainties (e.g., Sanogo et al., 2022). It reveals that in regions regularly affected by TSs and TCs, only 10%–30% of EPEs are directly linked to these weather systems, except in Reunion where 55% are cyclonic on average, up to 60%–80% on its relief. Our results are comparable with the global study of Prat and Nelson (2016). However, rain gauges provide greater precision compared to satellite products. TSs contribute the most to cyclonic EPEs and the EPE probability of occurrence is shown to increase during cyclonic days by a factor of 4–15, depending on the territory. Also, in most territories, the EPE frequency of occurrence increases from TSs, weak TCs to more intense TC categories. Understanding better the physical processes driving TCs' behavior and heavy rainfall during cyclonic days requires further investigation.

Among the diversity of sampled tropical environments, EPEs not associated with TCs are found to occur within a large-scale and intense moist atmospheric envelope of enhanced convection accompanied by anomalous cyclonic circulations driving an anomalous moist low-level flow from the Equator to the subtropical latitudes. On average, the intraseasonal timescale contributes the most to the total anomalies. And, during non-cyclonic EPEs, the large-scale environment is characterized by a convectively active phase of an intense intraseasonal event, possibly linked with CCEWs or mid-latitude Rossby waves propagating equatorward. Even if their contribution is weaker, the seasonal-to-annual and interannual timescales significantly add to the total moist and convective anomalies. These scales cannot trigger EPEs alone but likely provide a favorable background environment to enhance intraseasonal events' effect. The evidence of these large-scale patterns, especially their intraseasonal component, provides opportunities to enhance the forecast skills of non-cyclonic EPEs over the tropics, with the monitoring of high-magnitude CCEWs and mid-latitude Rossby waves.

Data Availability Statement

All data used in this manuscript are publicly and freely available. Daily rain gauge data in the French Overseas territories provided by Meteo-France are now available from the website https://meteo.data.gouv.fr/datasets/6569b51ae64326786e4e8e1a. National Oceanic and Atmospheric Administration Interpolated OLR data

provided by the NOAA PSL, Boulder, Colorado, USA, from their website at https://psl.noaa.gov/data/gridded/data.olrcdr.interp.html. How to download the ERA5 reanalysis data is accessible at the ECMWF website: https://confluence.ecmwf.int/display/CKB/How+to+download+ERA5.

Acknowledgments
Meteo-France forecasters and climatologists in the different French Overseas territories are acknowledged for our stimulating discussions during this work. Special thanks are also addressed to the Meteo-France IT support.

References

Ajayamohan, R. S., & Rao, S. A. (2008). Indian Ocean dipole modulates the number of extreme rainfall events over India in a warming environment. *Journal of the Meteorological Society of Japan. Ser. II*, *86*(1), 245–252. https://doi.org/10.2151/jmsj.86.245

Alexander, L. V., Bador, M., Roca, R., Contractor, S., Donat, M. G., & Nguyen, P. L. (2020). Intercomparison of annual precipitation indices and extremes over global land areas from in situ, space-based and reanalysis products. *Environmental Research Letters*, *15*(5), 055002. https://doi.org/10.1088/1748-9326/ab79e2

Alexander, L. V., Fowler, H. J., Bador, M., Behrangi, A., Donat, M. G., Dunn, R., et al. (2019). On the use of indices to study extreme precipitation on sub-daily and daily timescales. *Environmental Research Letters*, *14*(12), 125008. https://doi.org/10.1088/1748-9326/ab51b6

Aoki, S., & Shige, S. (2023). Control of low-level wind on the Diurnal cycle of tropical coastal precipitation. *Journal of Climate*, *37*(1), 229–247. https://doi.org/10.1175/JCLI-D-23-0180.1

Bagtasa, G. (2017). Contribution of tropical cyclones to rainfall in the Philippines. *Journal of Climate*, *30*(10), 3621–3633. https://doi.org/10.1175/JCLI-D-16-0150.1

Behera, S. K., & Yamagata, T. (2001). Subtropical SST dipole events in the southern Indian Ocean. *Geophysical Research Letters*, *28*(2), 327–330. https://doi.org/10.1029/2000GL011451

Brown, J. R., Lengaigne, M., Lintner, B. R., Widlansky, M. J., van der Wiel, K., Dutheil, C., et al. (2020). South Pacific Convergence Zone dynamics, variability and impacts in a changing climate. *Nature Reviews Earth & Environment*, *1*(10), 530–543. https://doi.org/10.1038/s43017-020-0078-2

Chen, L.-s. (2012). Research progress on the structure and intensity change for the landfalling tropical cyclones. *Journal of Tropical Meteorology*, *18*(2), 6. https://doi.org/10.3969/j.issn.1006-8775.2012.02.001

CRED and UNDRR. (2020). *The human cost of disasters: An overview of the last 20 years (2000-2019)* (Tech. Rep.). Centre for Research on the Epidemiology of Disasters (CRED).

Dai, N., & Soden, B. J. (2020). Convective aggregation and the amplification of tropical precipitation extremes. *AGU Advances*, *1*(4), e2020AV000201. https://doi.org/10.1029/2020AV000201

Deo, A., Chand, S. S., Ramsay, H., Holbrook, N. J., McGree, S., Magee, A., et al. (2021). Tropical cyclone contribution to extreme rainfall over southwest Pacific Island nations. *Climate Dynamics*, *56*(11), 3967–3993. https://doi.org/10.1007/s00382-021-05680-5

Duchon, C. E. (1979). Lanczos filtering in one and two dimensions. *Journal of Applied Meteorology and Climatology*, *18*(8), 1016–1022. https://doi.org/10.1175/1520-0450(1979)018⟨1016:LFIOAT⟩2.0.CO;2

Efron, B. (1979). Bootstrap methods: Another look at the Jackknife. *Annals of Statistics*, *7*(1), 1–26. https://doi.org/10.1214/aos/1176344552

European Space Agency and Sinergise. (2021). Copernicus global digital surface model [dataset]. *OpenTopography*. https://doi.org/10.5069/G9028PQB

Ferrett, S., Yang, G.-Y., Woolnough, S. J., Methven, J., Hodges, K., & Holloway, C. E. (2020). Linking extreme precipitation in Southeast Asia to equatorial waves. *Quarterly Journal of the Royal Meteorological Society*, *146*(727), 665–684. https://doi.org/10.1002/qj.3699

Hersbach, H., Bell, B., Berrisford, P., Hirahara, S., Horányi, A., Muñoz-Sabater, J., et al. (2020). The ERA5 global reanalysis [dataset]. *Quarterly Journal of the Royal Meteorological Society*, *146*(730), 1999–2049. https://doi.org/10.1002/qj.3803

Hoell, A., & Cheng, L. (2018). Austral summer Southern Africa precipitation extremes forced by the El Niño-Southern oscillation and the subtropical Indian Ocean dipole. *Climate Dynamics*, *50*(9), 3219–3236. https://doi.org/10.1007/s00382-017-3801-z

Khouakhi, A., Villarini, G., & Vecchi, G. A. (2017). Contribution of tropical cyclones to rainfall at the global scale. *Journal of Climate*, *30*(1), 359–372. https://doi.org/10.1175/JCLI-D-16-0298.1

Kiladis, G. N., Wheeler, M. C., Haertel, P. T., Straub, K. H., & Roundy, P. E. (2009). Convectively coupled equatorial waves. *Reviews of Geophysics*, *47*(2). https://doi.org/10.1029/2008RG000266

Kim, S., Sharma, A., Wasko, C., & Nathan, R. (2022). Linking total precipitable water to precipitation extremes globally. *Earth's Future*, *10*(2), e2021EF002473. https://doi.org/10.1029/2021EF002473

Knapp, K. R., Kruk, M. C., Levinson, D. H., Diamond, H. J., & Neumann, C. J. (2010). The international best track archive for climate stewardship (IBTrACS): Unifying tropical cyclone data [dataset]. *Bulletin of the American Meteorological Society*, *91*(3), 363–376. https://doi.org/10.1175/2009BAMS2755.1

Knight, D. B., & Davis, R. E. (2009). Contribution of tropical cyclones to extreme rainfall events in the southeastern United States. *Journal of Geophysical Research*, *114*(D23), 2009JD012511. https://doi.org/10.1029/2009JD012511

Kunkel, K. E., Easterling, D. R., Kristovich, D. A., Gleason, B., Stoecker, L., & Smith, R. (2010). Recent increases in U.S. heavy precipitation associated with tropical cyclones. *Geophysical Research Letters*, *37*(24). https://doi.org/10.1029/2010GL045164

Kunkel, K. E., Stevens, S. E., Stevens, L. E., & Karl, T. R. (2020). Observed climatological relationships of extreme daily precipitation events with precipitable water and vertical velocity in the contiguous United States. *Geophysical Research Letters*, *47*(12), e2019GL086721. https://doi.org/10.1029/2019GL086721

Lafore, J.-P., Beucher, F., Peyrillé, P., Diongue-Niang, A., Chapelon, N., Bouniol, D., et al. (2017). A multi-scale analysis of the extreme rain event of Ouagadougou in 2009. *Quarterly Journal of the Royal Meteorological Society*, *143*(709), 3094–3109. https://doi.org/10.1002/qj.3165

Latos, B., Lefort, T., Flatau, M. K., Flatau, P. J., Permana, D. S., Baranowski, D. B., et al. (2021). Equatorial waves triggering extreme rainfall and floods in Southwest Sulawesi, Indonesia. *Monthly Weather Review*, *149*(5), 1381–1401. https://doi.org/10.1175/MWR-D-20-0262.1

Liebmann, B., & Smith, C. (1996). Description of a complete (interpolated) outgoing longwave radiation dataset. *Bulletin of the American Meteorological Society*, *77*(6), 1275–1277.

Lubis, S. W., & Respati, M. R. (2021). Impacts of convectively coupled equatorial waves on rainfall extremes in Java, Indonesia. *International Journal of Climatology*, *41*(4), 2418–2440. https://doi.org/10.1002/joc.6967

MacLeod, D., Easton-Calabria, E., de Perez, E. C., & Jaime, C. (2021). Verification of forecasts for extreme rainfall, tropical cyclones, flood and storm surge over Myanmar and the Philippines. *Weather and Climate Extremes*, *33*, 100325. https://doi.org/10.1016/j.wace.2021.100325

Mann, H. B., & Whitney, D. R. (1947). On a test of whether one of two random variables is stochastically larger than the other. *The Annals of Mathematical Statistics*, *18*(1), 50–60. https://doi.org/10.1214/aoms/1177730491

McPhaden, M. J., Santoso, A., & Cai, W. (2020). Introduction to El Niño Southern Oscillation in a changing climate. In *El Niño Southern Oscillation in a changing climate* (pp. 1–19). American Geophysical Union (AGU). https://doi.org/10.1002/9781119548164.ch1

Muller, A., Reason, C. J. C., & Fauchereau, N. (2008). Extreme rainfall in the Namib desert during late summer 2006 and influences of regional ocean variability. *International Journal of Climatology*, *28*(8), 1061–1070. https://doi.org/10.1002/joc.1603

Pariyar, S. K., Keenlyside, N., Sorteberg, A., Spengler, T., Chandra Bhatt, B., & Ogawa, F. (2020). Factors affecting extreme rainfall events in the South Pacific. *Weather and Climate Extremes*, *29*, 100262. https://doi.org/10.1016/j.wace.2020.100262

Peyrillé, P., Roehrig, R., & Sanogo, S. (2023). Tropical waves are key drivers of extreme precipitation events in the Central Sahel. *Geophysical Research Letters*, *50*(20), e2023GL103715. https://doi.org/10.1029/2023GL103715

Prat, O. P., & Nelson, B. R. (2013). Mapping the world's tropical cyclone rainfall contribution over land using the TRMM Multi-satellite Precipitation Analysis. *Water Resources Research*, *49*(11), 7236–7254. https://doi.org/10.1002/wrcr.20527

Prat, O. P., & Nelson, B. R. (2016). On the link between tropical cyclones and daily rainfall extremes derived from global satellite observations. *Journal of Climate*, *29*(17), 6127–6135. https://doi.org/10.1175/JCLI-D-16-0289.1

Rapolaki, R. S., Blamey, R. C., Hermes, J. C., & Reason, C. J. C. (2019). A classification of synoptic weather patterns linked to extreme rainfall over the Limpopo River Basin in southern Africa. *Climate Dynamics*, *53*(3), 2265–2279. https://doi.org/10.1007/s00382-019-04829-7

Roca, R., Aublanc, J., Chambon, P., Fiolleau, T., & Viltard, N. (2014). Robust observational quantification of the contribution of mesoscale convective systems to rainfall in the tropics. *Journal of Climate*, *27*(13), 4952–4958. https://doi.org/10.1175/JCLI-D-13-00628.1

Roca, R., & Fiolleau, T. (2020). Extreme precipitation in the tropics is closely associated with long-lived convective systems. *Communications Earth & Environment*, *1*(1), 18. https://doi.org/10.1038/s43247-020-00015-4

Roderick, T. P., Wasko, C., & Sharma, A. (2019). Atmospheric moisture measurements explain increases in tropical rainfall extremes. *Geophysical Research Letters*, *46*(3), 1375–1382. https://doi.org/10.1029/2018GL080833

Roderick, T. P., Wasko, C., & Sharma, A. (2020). An improved covariate for projecting future rainfall extremes? *Water Resources Research*, *56*(8), e2019WR026924. https://doi.org/10.1029/2019WR026924

Saji, N. H., Goswami, B. N., Vinayachandran, P. N., & Yamagata, T. (1999). A dipole mode in the tropical Indian Ocean. *Nature*, *401*(6751), 360–363. https://doi.org/10.1038/43854

Sanogo, S., Peyrillé, P., Roehrig, R., Guichard, F., & Ouedraogo, O. (2022). Extreme precipitating events in satellite and rain gauge products over the Sahel. *Journal of Climate*, *35*(6), 1915–1938. https://doi.org/10.1175/JCLI-D-21-0390.1

Schreck, C. J., III. (2021). Global survey of the MJO and extreme precipitation. *Geophysical Research Letters*, *48*(19), e2021GL094691. https://doi.org/10.1029/2021GL094691

Semie, A. G., & Bony, S. (2020). Relationship between precipitation extremes and convective organization inferred from satellite observations. *Geophysical Research Letters*, *47*(9). https://doi.org/10.1029/2019GL086927

Serra, Y. L., Jiang, X., Tian, B., Amador-Astua, J., Maloney, E. D., & Kiladis, G. N. (2014). Tropical intraseasonal modes of the atmosphere. *Annual Review of Environment and Resources*, *39*(1), 189–215. https://doi.org/10.1146/annurev-environ-020413-134219

Ta, S., Kouadio, K. Y., Ali, K. E., Toualy, E., Aman, A., & Yoroba, F. (2016). West Africa extreme rainfall events and large-scale ocean surface and atmospheric conditions in the tropical Atlantic. *Advances in Meteorology*, *2016*, 19404566. https://doi.org/10.1155/2016/1940456

Villarini, G., & Denniston, R. F. (2016). Contribution of tropical cyclones to extreme rainfall in Australia. *International Journal of Climatology*, *36*(2), 1019–1025. https://doi.org/10.1002/joc.4393

Vogel, P., Knippertz, P., Fink, A. H., Schlueter, A., & Gneiting, T. (2020). Skill of global raw and postprocessed ensemble predictions of rainfall in the tropics. *Weather and Forecasting*, *35*(6), 2367–2385. https://doi.org/10.1175/WAF-D-20-0082.1

Wang, S., & Sobel, A. H. (2017). Factors controlling rain on small tropical islands: Diurnal cycle, large-scale wind speed, and topography. *Journal of the Atmospheric Sciences*, *74*(11), 3515–3532. https://doi.org/10.1175/JAS-D-16-0344.1

Welch, B. L. (1947). The generalization of 'Student's' problem when several different population variances are involved. *Biometrika*, *34*(1–2), 28–35. https://doi.org/10.1093/biomet/34.1-2.28

Woodhams, B. J., Birch, C. E., Marsham, J. H., Bain, C. L., Roberts, N. M., & Boyd, D. F. A. (2018). What is the added value of a convection-permitting model for forecasting extreme rainfall over tropical East Africa? *Monthly Weather Review*, *146*(9), 2757–2780. https://doi.org/10.1175/MWR-D-17-0396.1

Zhao, M. (2022). A study of AR-TS-and MCS-associated precipitation and extreme precipitation in present and warmer climates. *Journal of Climate*, *35*(2), 479–497. https://doi.org/10.1175/JCLI-D-21-0145.1